Supporting Information

Skeletal double gyroid formed by single coaxial bundles of catechol based bolapolyphiles

Silvio Poppe,[+,a] Changlong Chen,[+,b] Feng Liu[b,*] and Carsten Tschierske[a,*]

[a] Institute of Chemistry, Martin-Luther-University Halle-Wittenberg, Kurt-Mothes-Straße 2, 06120 Halle

[b] State Key Laboratory for Mechanical Behaviour of Materials, Xi'an Jiaotong University, Xi'an 710049 (P.R. China)

1. Methods

Optical and calorimetric investigations. Phase transitions were determined by polarizing microscopy (Leica DMR XP) in conjunction with a heating stage (FP 82 HT, Mettler) and controller (FP 90, Mettler) and by differential scanning calorimetry (DSC-7, Perkin Elmer) at heating/cooling rates of 10 K min^{-1} (peak temperatures). Optical investigation was carried out under equilibrium conditions between glass slides which were used without further treatment, sample thickness was ~15 µm. A full wavelength retardation plate was used to determine the sign of birefringence.

X-ray diffraction. X-ray investigations (Kristalloflex 760H, Siemens) were carried out using Ni filtered CuKα radiation (15 to 30 min exposure time). Aligned samples were obtained on a glass plate. Alignment was achieved upon slow cooling (rate: 1 K min^{-1} – 0.01 K min^{-1}) of a small droplet of the sample. The aligned samples were held on a temperature controlled heating stage and the diffraction patterns were recorded with a 2D detector (Vantec 500, Bruker). The sample-detector distance for the samples was 9.00 cm for WAXD and 26.70 cm for SAXD measurements.

Synchrotron X-ray diffraction and electron density reconstruction.- High-resolution small-angle powder diffraction experiments were recorded on Beamline BL16B1 at Shanghai Synchrotron Radiation Facility, SSRF. Samples were held in evacuated 1 mm capillaries. A modified Linkam hot stage with a thermal stability within 0.2 ºC was used, with a hole for the capillary drilled through the silver heating block and mica windows attached to it on each side. A MarCCD detector was used. q calibration and linearization were verified using several orders of layer reflections from silver behemate and a series of n-alkanes. The measurement of the positions and intensities of the diffraction peaks is carried out using Galactic PeakSolve^{TM} program, where experimental diffractograms are fitted using Gaussian shaped peaks. The diffraction peaks are indexed on the basis of their peak positions, and the lattice parameters and the space groups are subsequently determined. Once the diffraction intensities are measured and the corresponding space group determined, 3-d electron density maps can be reconstructed, on the basis of the general formula

$$E(xyz) = \Sigma_{hkl} \, F(hkl) \, \exp[i2\pi(hx+ky+lz)] \qquad \text{(Eqn. 1)}$$

Here $F(hkl)$ is the structure factor of a diffraction peak with index (hkl). It is normally a complex number and the experimentally observed diffraction intensity

$$I(hkl) = K \cdot F(hkl) \cdot F^*(hkl) = K \cdot |F(hkl)|^2 \qquad \text{(Eqn. 2)}$$

Here K is a constant related to the sample volume, incident beam intensity etc. In this paper we are only interested in the relative electron densities, hence this constant is simply taken to be 1. Thus the electron density

$$E(xyz) = \Sigma_{hkl} \text{ sqrt}[I(hkl)] \exp[i2\pi(hx+ky+lz)+\phi_{hkl}] \qquad \text{(Eqn. 3)}$$

As the observed diffraction intensity $I(hkl)$ is only related to the amplitude of the structure factor $|F(hkl)|$, the information about the phase of $F(hkl)$, ϕ_{hkl}, can not be determined directly from experiment. However, the problem is much simplified when the structure of the ordered phase is centrosymmetric, and hence the structure factor $F(hkl)$ is always real and ϕ_{hkl} is either 0 or π.

This makes it possible for a trial-and-error approach, where candidate electron density maps are reconstructed for all possible phase combinations, and the "correct" phase combination is then selected on the merit of the maps, helped by prior physical and chemical knowledge of the system. This is especially useful for the study of nanostructures, where normally only a limited number of diffraction peaks are observed.
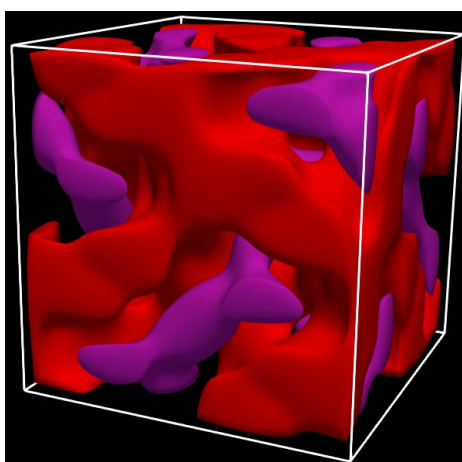
2. Additional Data
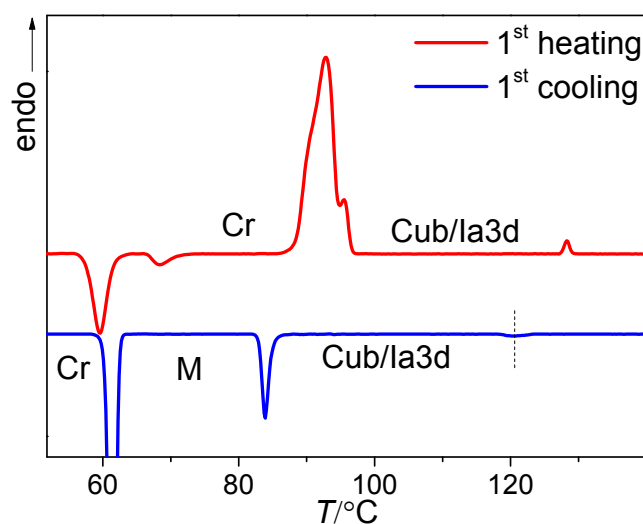

Figure S1. DSC traces of compound **1** (rate 10 K min^{-1}).
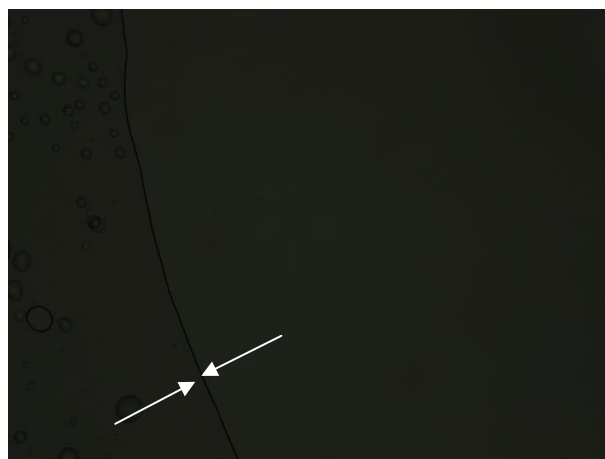
Figure S2. Texture of the Cub/$Ia\bar{3}d$ phase of compound **1** at T = 100 °C; the arrows indicate the position of the boundary to air.

Figure S3. 3D two-colour contour electron density map of Cub/$Ia\bar{3}d$ phase of compound **1**. The purple isoelectron surfaces enclose the aromatic cores and the glycerol groups (high electron density) and the red surfaces enclose the alkyl chains (low electron density).
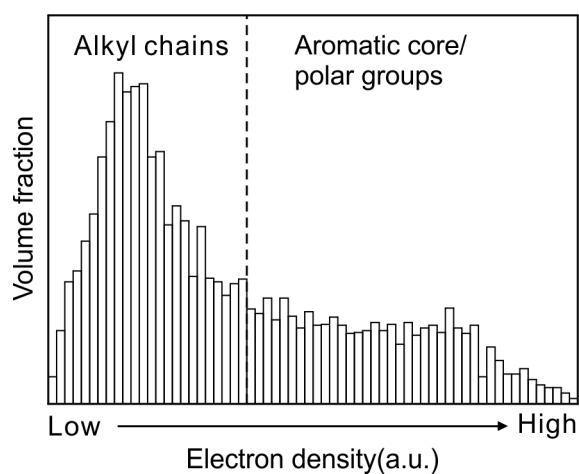
Figure S4. The electron density histogram of the Cub/$Ia\bar{3}d$ phase of compound **1**, calculated based on the phase combination corresponding to Figures 3c and S3. The calculated volume ratio is 0.61:0.39 for alkyl chains and (aromatic + glycerol) groups, respectively.
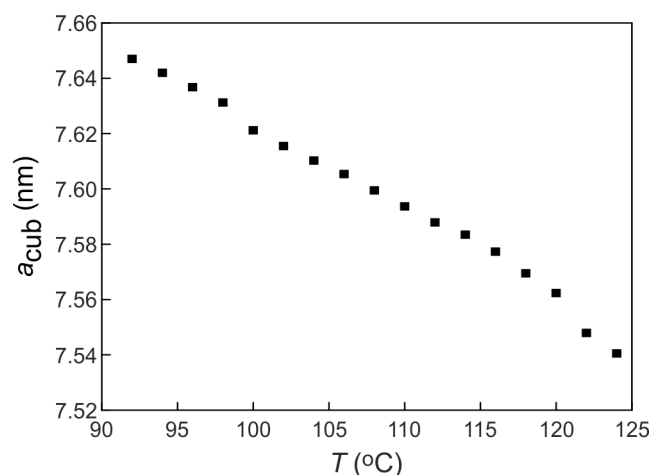
Figure S5. The temperature dependence of the lattice parameter of the Cub/$Ia\bar{3}d$ phase.

Table S1: Experimental and calculated d-spacings of the observed SAXS reflections of the Cubic phase Cub/$Ia\bar{3}d$ phase in **1** at 100 ºC. All intensity values are Lorentz and multiplicity corrected.

(*hkl*)	$d_{obs.}$ – spacing (nm)	$d_{cal.}$ – spacing (nm)	*intensity*	*phase*
(211)	3.12	3.12	100.0	π
(220)	2.70	2.70	5.9	π
(321)	2.04	2.04	0.7	0
(400)	1.91	1.91	9.3	π
(420)	1.71	1.71	4.5	π
(332)	1.63	1.63	0.8	0
(422)	1.56	1.56	3.4	0
(431)	1.50	1.50	0.3	0
(440)	1.35	1.35	1.6	0
a_{cub} = 7.76 nm				

Table S2: Calculations of molecules per unit cell for Cub/$Ia\bar{3}d$ phase of compound **1**, a_{cub} − lattice parameter, L_{mol} − molecular length, V_{mol} − volume of molecule (determined from the increment system of Immirzi[S1]), V_{cell} − volume of unit cell, n_{cr} − number of molecules in crystalline state, n_{liq} − number of molecules in liquid state, n_{cell} − number of molecules in liquid crystalline state, $d_{k\mathrm{nots}}$ − distance between two junctions, n_{bundle} − number of molecules of one bundle.

a_{cub} / nm	7.76
L_{mol} / nm	2.5
V_{mol} /nm^3	1.44
V_{cell} / nm^3	467
n_{cr}	324
n_{liq}	255
n_{cell}	290
$d_{k\mathrm{nots}}$ / nm	2.74
n_{bundle}	12

Table S3: Calculations of $V_{\mathrm{chain}}/L_{\mathrm{mol}}$[a]

Compound No.	V_{chain} (nm^3)	L_{mol} (nm)	V_{chain} / L_{mol}
1	0.69	2.5	0.28
2[b]	1.05	1.9	0.55
3[b]	1.68	2.5	0.67

[a] V_{chain} and L_{mol} were calculated by using Material Studio (Accelrys), respecvtively; [b] phase transition temperatures (T/°C) and transition enthalpies [ΔH/kJ mol^{-1}]:
2: Cr 108 [45.3] Lam$_{\mathrm{Sm}}$ 132 Lam$_{\mathrm{N}}$ 133 [5.66][c] Col$_{\mathrm{rec}}$/$c2mm$ 145 [1.88] Cub/$Ia3d$ 178 [1.33] Iso; **3**: Cr 83 [22.9] Col$_{\mathrm{hex}}$ 175 [11.7] Iso; [c] both transitions not resolved

3. Synthesis and Analytical Data

3.1 General

Unless otherwise noted, all starting materials were purchased from commercial sources and were used without further purification. Column chromatography was performed with silica gel 60 (63-200 μm, Fluka). Determination of structures and purity of intermediates and products was obtained by NMR spectroscopy (VARIAN Gemini 2000 and Unity Inova 500, all spectra were recorded at 27 °C). Microanalyses were performed using a CARLO Erba-CHNO 1102 elemental analyzer and a micrOTOF HR-ESI mass spectrometer (Bruker). The purity of all products was checked with thin layer chromatography (silicagel 60 F_{254}, Merck). $CHCl_3$ and $CHCl_3$/MeOH mixtures were used as eluents and the spots were detected by UV radiation. The synthesis of 1,4-diiodo-2,3-dihydroxybenzene is described in the ref.[S2]. 4-((2,2-Dimethyl-1,3-dioxolan-4-yl)methoxy)phenylboronic acid was synthesized as reported in ref.[S3] 1-Bromooctadecasne is commercially available from Sigma Aldrich.

3.2. Synthesis

2,3-Dioctadecyloxy-1,4-diiodobenzene: Synthesized according to the ref.[S2] from 1,4-diiodo-2,3-dihydroxybenzene (250 mg, 0.69 mmol), 1-bromooctadecane (510 mg, 1.52 mmol), K_2CO_3 (960 mg, 6.90 mmol), Bu_4NI (10 mg, 0.03 mmol) in DMF (30 mL). purification by column chromatography (eluent: *n*-hexane/$CHCl_3$ = 4/1), white solid, $C_{42}H_{76}I_2O_2$, M = 866.86 g/mol, yield: 590 mg (95%), mp. 79 °C, ^{1}H-NMR (CDCl$_3$, 400 MHz): δ/ppm = 7.22 (s, 2H, Aryl-*H*), 3.98 (t, $^3J_{H,H}$ = 6.7 Hz, 4H, OC*H$_2$*), 1.89 – 1.77 (m, 4H, C*H$_2$*), 1.52 – 1.44 (m, 4H, C*H$_2$*), 1.41 – 1.21 (m, 56H, -C*H$_2$*), 0.89 (t, $^3J_{H,H}$ = 6.8 Hz, 6H, C*H$_3$*).

2,2′-*n*-Octadecyloxy-4,4′′-bis[(2,2-dimethyl-1,3-dioxolan-4-yl)methoxy]-*p*-terphenyl (4): 2,3-Dioctadecyloxy-1,4-diiodobenzene (590 mg, 0.68 mmol),4-((2,2-dimethyl-1,3-dioxolan-4-yl)methoxy)benzene boronic acid (430 mg, 1.70 mmol), [Pd(PPh$_3$)$_4$] (50 mg, 0.03 mmol), sat. NaHCO$_3$-sol. (20 mL) in THF (30 mL) was heated to reflux for 5 h. Afterwards the mixture was extracted with EtOAc (3x50 mL) and the organic layer was washed with water and brine. The solvent was removed under reduced pressure and the residue was purified by column chromatography (eluent: CHCl$_3$). Colorless solid, $C_{66}H_{106}O_8$, M = 1027.54 g/mol,

yield: 300 mg (43%), mp. 43 °C, **^{1}H-NMR** (CDCl$_3$, 400 MHz): δ/ppm = 7.54 – 7.48 (m, 4H, Aryl-*H*), 7.08 (s, 2H, Aryl-*H*), 6.98 – 6.92 (m, 4H, Aryl-*H*), 4.51 (quin, $^3J_{H,H}$ = 5.97 Hz, 2H, OC*H*), 4.19 (dd, $^3J_{H,H}$ = 8.5, $^3J_{H,H}$ = 6.4 Hz, 2H, OC*H$_2$*), 4.16 – 4.08 (m, 2H, OC*H$_2$*), 4.04 – 3.90 (m, 4H, OC*H$_2$*), 3.76 (t, $^3J_{H,H}$ = 6.5 Hz, 4H, OC*H$_2$*), 1.58 – 1.50 (m, 4H, C*H$_2$*), 1.48 (s, 6H, OC(C*H$_3$*)$_2$), 1.42 (s, 6H, OC(C*H$_3$*)$_2$), 1.35 – 1.13 (m, 60H, CH$_2$), 0.88 (t, $^3J_{H,H}$ = 6.9 Hz, 6H, C*H$_3$*).

2, 2′-Di-*n*-Octadecyoxyl-4,4′′-bis(2,3-dihydroxypropyloxy)-*p*-terphenyl (1): A mixture of **4** (300 mg, 0.40 mmol); HCl (10%, 5 mL) in MeOH (20 mL) and THF (20 mL) was stirred at reflux for 6 h. Afterwards the mixture was extracted with EtOAc (3x50 mL) and the organic phase was washed with saturated NaHCO$_3$-sol. (20 mL), water (20 mL) and brine (20 mL). After drying over Na$_2$SO$_4$ the solvent was removed under reduced pressure and the residue was purified by column chromatography (eluent: CHCl$_3$/MeOH = 9/1) and recrystallized from MeOH. Colorless solid, C$_{60}$H$_{98}$O$_8$, *M* = 947.42 g/mol, yield: 250 mg (90%), Cr 93 Cub 128 Iso (°C), ^{1}H NMR (pyridine-d$_5$, 400 MHz): δ/ppm 7.83 (d, $^3J_{H,H}$ = 8.7 Hz, 4H, Aryl-*H*), 7.35 (s, 2H, Aryl-*H*), 7.29 (d, $^3J_{H,H}$ = 8.7 Hz, 4H, Aryl-*H*), 4.62 (m, 4H, OC*H$_2$*), 4.52 (m, 2H, OC*H*), 4.34 – 4.22 (m, 4H, OC*H$_2$*), 4.04 (t, $^3J_{H,H}$ = 6.5 Hz, 4H, OC*H$_2$*), 1.81 – 1.68 (m, 4H, C*H$_2$*), 1.49 – 1.36 (m, 4H, C*H$_2$*), 1.2-1.5 (m, 60H, C*H$_2$*), 0.89 (t, $^3J_{H,H}$ = 6.8 Hz, 6H, C*H$_3$*). ^{13}C NMR (pyridine-d$_5$, 101 MHz): δ/ppm = 157.80, 149.75, 129.84, 129.55, 124.38, 113.38 (Aryl-*C*), 72.34, 70.10, 69.59 (OC*H$_2$*), 63.00 (OC*H*), 30.70, 29.29, 28.62, 28.59, 28.57, 28.51, 28.38, 28.19, 25.06, 21.51 (*C*H$_2$), 12.85 (*C*H$_3$). HRMS (*m/z*): [M]+Cl$^-$; calcd. for C$_{60}$H$_{98}$O$_8$Cl, 981.6945; found 981.6895 g/mol.
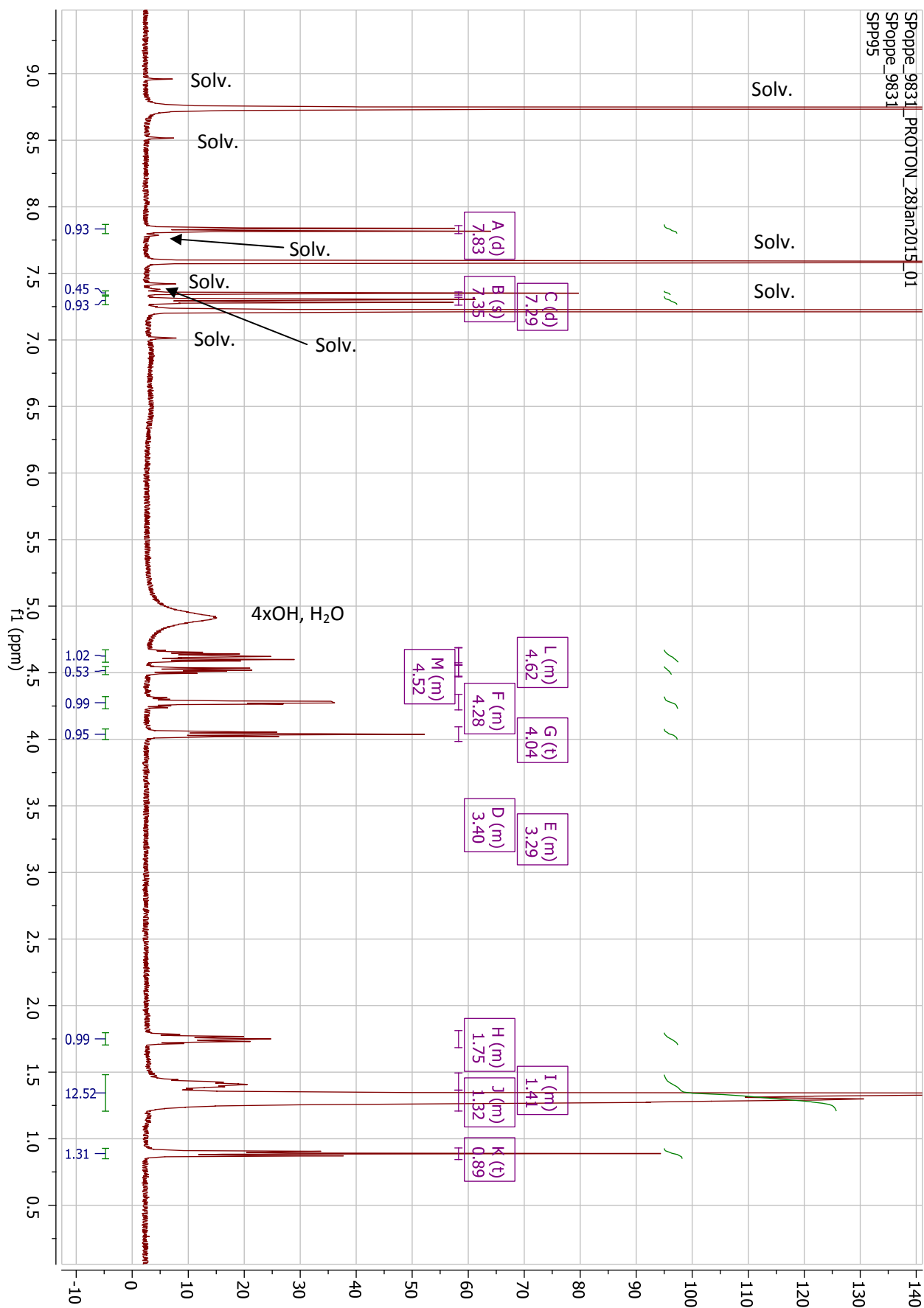
Figure S6: ^{1}H NMR (pyridine-d$_5$, 400 MHz) of compound **1** at 27 °C (all 6 small peaks in the aromatic region are rotational side bands of the 3 strong solvent signals).
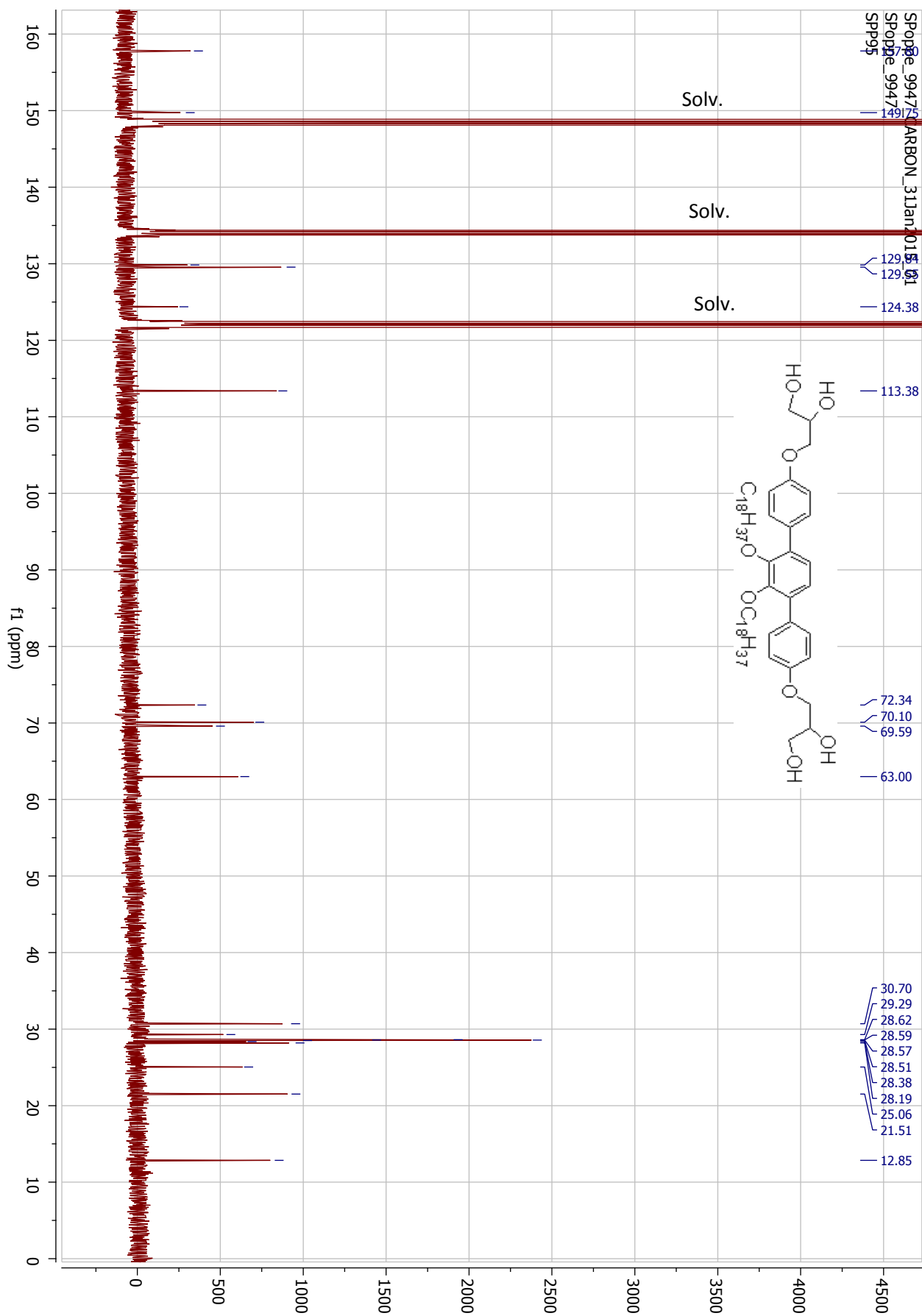
Figure S7: ^{13}C NMR (pyridine-d_5, 101 MHz) of compound **1** at 27 °C..

4. References

[S1] A. Immirzi, B. Perini, *Acta Cryst*. **1977**, *33*, 216-218.

[S2] Z. Zhu, T. M. Swager, *Org. Lett*. **2001**, *3*, 3471–3474.

[S3] M. Kölbel,, T. Beyersdorff, X. Cheng, C. Tschierske, J. Kain, S. Diele,. *J. Am. Chem. Soc.* **2001**, *123*, 6809-6818.